

Tennessee State University

## Digital Scholarship @ Tennessee State University

---

Mathematical Sciences Faculty Research

Department of Mathematical Sciences

---

1-26-2011

### Ab initio investigation of hydrogen bonding and network structure in a supercooled model of water

Lei Liang

*University of Missouri-Kansas City*

Paul Rulis

*University of Missouri-Kansas City*

Lizhi Ouyang

*Tennessee State University*

Wai-Yim Ching

*University of Missouri-Kansas City*

Follow this and additional works at: <https://digitalscholarship.tnstate.edu/mathematics>

 Part of the [Chemistry Commons](#)

---

#### Recommended Citation

L. Liang, P. Rulis, L. Ouyang, W.Y. Ching "Ab initio investigation of hydrogen bonding and network structure in a supercooled model of water" *Phys. Rev. B* 83, 024201 (2011) <https://doi.org/10.1103/PhysRevB.83.024201>

This Article is brought to you for free and open access by the Department of Mathematical Sciences at Digital Scholarship @ Tennessee State University. It has been accepted for inclusion in Mathematical Sciences Faculty Research by an authorized administrator of Digital Scholarship @ Tennessee State University. For more information, please contact [XGE@Tnstate.edu](mailto:XGE@Tnstate.edu).



# CHORUS

This is the accepted manuscript made available via CHORUS. The article has been published as:

## Ab initio investigation of hydrogen bonding and network structure in a supercooled model of water

Lei Liang, Paul Rulis, Lizhi Ouyang, and W. Y. Ching

Phys. Rev. B **83**, 024201 — Published 26 January 2011

DOI: [10.1103/PhysRevB.83.024201](https://doi.org/10.1103/PhysRevB.83.024201)

# *Ab initio* Investigation of H-bonding and Network Structure in a Super-cooled Model of Water

Lei Liang,<sup>1</sup> Paul Rulis,<sup>1</sup> Lizhi Ouyang,<sup>2</sup> and W.Y. Ching<sup>1</sup>

1. Department of Physics, University of Missouri-Kansas City, Kansas City, MO, 64110
2. Department of Mathematics and Physics, Tennessee State University, Nashville, TN, 37209

## Abstract

The hydrogen bond (HB) and network structure in a large periodic model of 340 water molecules are investigated by *ab initio* methods. This model has a density of 1.00 g/cc, very small distortions of O-H bond length and H-O-H bond angle, and the peak positions in the radial distribution functions in close agreement with experiment. The 340 molecules can be classified into four groups according to the number of HBs quantitatively determined by the bond order values. The percentages of water molecules with 2, 3, 4, and 5 HBs are respectively 3.2%, 10.3%, 85% and 1.5% with an average HB number per H<sub>2</sub>O of 3.85 which clearly supports the tetrahedral network description for this model. The O-K edges of the X-ray absorption near edge structure of every water molecule are calculated by the *ab initio* supercell orthogonalized linear combination of atomic orbitals method. Statistical analysis of the calculated O-K edge spectra shows that the experimentally observed pre-peak originates predominately from H<sub>2</sub>O molecules with two HBs and that there exist large fluctuations in the spectral features of individual water molecules within a given set.

(PACS No: 82.30.Rs, 61.20.Gy, 61.05.cj, 61.20.Ja)

(Key words: water, *ab initio* calculation, Hydrogen Bond, Oxygen XANES)

## I. INTRODUCTION

Water is one of the most common and intriguing substances on Earth yet it is far from being fully understood. In addition to the liquid and vapor phases, there exist many phases of solid H<sub>2</sub>O covering a wide range of temperatures and pressures that exhibit many interesting phenomena. All the properties of these phases are closely related to the local configurations of the water molecules as determined by their intermolecular interactions – especially their hydrogen bonds (HBs).<sup>1</sup> The existence of a network structure of H<sub>2</sub>O in the liquid phase is a fundamental issue that has attracted a lot of attention both experimentally and theoretically. Due to the variety of existing models of water, the limitations of experimental techniques to verify them, the need for precise criteria to define a HB, and the lack of unambiguous criteria to analyze them, there are conflicting opinions as to whether the molecules in water form a network structure primarily composed of tetrahedrally bonded H<sub>2</sub>O or of one dimensional filamentous structures.<sup>2-7</sup> Several models regarding the network characteristics have been proposed to interpret experimental neutron scattering and x-ray absorption near edge structure (XANES) spectral data.<sup>2, 8</sup> On the theoretical side, models with non-periodic clusters ranging from several to a few hundred molecules have been studied using different first principles computational methods including *ab*

*initio* molecular dynamics (MD) and density functional theory (DFT).<sup>9-11</sup> There have also been discussions that the ambient condition simulations using DFT functionals will describe a supercooled state that is overstructured compared to liquid water.<sup>12</sup>

In this paper, we report a detailed *ab initio* simulation of a large realistic periodic model of bulk water with 340 molecules at ambient conditions along with the calculation of the O-K edges of the XANES spectra of *all* the water molecules in the model. By using a precisely defined HB definition, based on quantum mechanical calculation of the bond order (BO) values for all the molecules in the model, we are able to present a statistical analysis of the HB network. We also show that quantitative BO values could be used to define appropriate geometric parameters for identifying the presence of hydrogen bonding in other models containing water. When the calculated O-K edge XANES spectra are accumulated we are able to accurately reproduce the observed experimental spectrum. Then, by analyzing the individual spectra we interpret the total XANES spectrum in terms of the HB configurations present in the model.

In the next section, we describe the construction of the water model and the computational methods used. The electronic structure results and hydrogen bonding properties are described in section III followed by a comparison of the calculated and measured XANES spectral results in section IV. The conclusions of this work are presented in the last section.

## II. MODEL CONSTRUCTION AND COMPUTATIONAL METHODS

To obtain a sufficiently large and valid model for bulk water a combination of different methods was applied. The first step was to construct an initial model with periodic boundary conditions and 340 water molecules ( $a = 21.6641\text{\AA}$ , density: 1g/cc) using Packmol.<sup>13</sup> The use of periodic boundary conditions eliminates the artificial surface effects that would be present when using finite molecular clusters. Next, we used the SIESTA code<sup>14</sup> for *ab initio* MD simulations to optimize the molecular system. The model was fully equilibrated at 300K for 3000 fs. It may be desirable to have a longer equilibrium time, but we believe that 3000 fs should be reasonably sufficient for the purposes of the present study. Snapshot configurations from the *ab initio* MD trajectory were selected and fully analyzed. Of these snapshots, the one with the most ideal configuration (identified by the absence of ionized species such as  $\text{OH}^-$  and  $\text{OH}_3^+$  ions) was chosen and its structure was fully relaxed using the Vienna *Ab initio* Simulation Package (VASP)<sup>15</sup> with high precision to minimize deviations of the O-H covalent bond length (BL) and H-O-H covalent bond angle (BA)  $\theta$  compared to the ideal  $\text{H}_2\text{O}$  molecule. The following VASP parameters were adopted: (1) the projector augmented-wave-PBE (PAW-PBE) potential<sup>16</sup> with the generalized gradient approximation (GGA); (2) a high energy cutoff of 500 eV; (3) an electronic convergence criterion of  $10^{-5}$  eV; (4) a force convergence criteria of  $10^{-3}$  eV/ $\text{\AA}$  for the ionic relaxation; and (5) one  $k$  point at  $\Gamma$  which is fully justified due to the large cell size and the correspondingly small Brillouin zone. In the *ab initio* calculation, each atom in the water molecule (O and H) is considered as an independent particle such that the short ranged interatomic interaction and the longer ranged intermolecular forces are treated on equal footing. The intermolecular forces determined in this way tend to allow the system to relax into the most favorable instantaneous configuration among many low energy possibilities. This is in sharp contrast with many MD simulations in which each  $\text{H}_2\text{O}$  molecule is treated as a fixed entity with only orientational and translational degrees of freedom. The above multi-step procedure for the

construction of the bulk water model is necessary to be able to obtain the most likely structure for bulk water at ambient conditions. A ball and stick picture of the final relaxed model is shown in Fig. 1.

The distribution of values for the bond lengths (BLs) and bond angles (BAs) is very narrow (Fig. 2) with small values for the standard deviations from the mean ( $1.00\pm 0.006$  Å and  $106.32^\circ\pm 2.528^\circ$  respectively). These values are very reasonable when compared to experimental data for liquid water.<sup>17</sup> When performing MD simulations where the atoms are treated as independent particles it is not generally necessary to minimize the BA and BL distortions because they are usually regarded as fluctuations and tend to be inconsequential when averaged over many configurations. However, for *ab initio* electronic structure calculations based on a *single model* this is generally not possible. An exceptionally large or unrealistic distortion in one or a few water molecules can adversely affect the quantum mechanical calculation of the electronic structure by introducing gap states. Figure 3 displays the calculated radial distribution functions (RDF) for the O-H, H-H, and O-O pairs along with neutron diffraction data.<sup>8</sup> The peak positions are in good agreement although, as expected, the peaks in the theoretical curves are much sharper, which has been discussed in the work by Yoo *et al.*<sup>12</sup> as a result of the supercooled state caused by the ambient condition MD DFT simulations. When the temperature rises to a much higher level than the ambient condition, the peak height reduces and becomes comparable to the experimental intensity.<sup>12</sup> Moreover, our single model simulation does not include the kinds of time dependent broadening effects associated with experimental measurements. The RDFs from MD simulations<sup>18</sup> are generally much broader and smoother because they are averaged over many configurations. Construction of more appropriate models for liquid water amenable for *ab initio* electronic studies aimed in the paper is beyond the scope of the current study.

Electronic structure calculations were then performed on the above model using the density functional theory-based orthogonalized linear combination of atomic orbitals (OLCAO) method with the local density approximation (LDA).<sup>19</sup> A full basis set of H (*1s*, *2s*, *2p*) and O (*1s*, *2s*, *2p*, *3s*, *3p*) was used to obtain the density of states (DOS) and partial DOS (PDOS). For the XANES calculation, the basis was further extended by one more shell of unoccupied atomic orbitals for more accurate determination of higher energy states. The supercell-OLCAO method for XANES calculation, which explicitly takes the core-hole effect into account, has been successfully applied to a large number of complex crystals, defects, surfaces, interfaces, and complex microstructures.<sup>20-25</sup> The detailed procedures for calculation of the XANES spectra have been reported elsewhere.<sup>26</sup> Hence we will describe only the essential concept for the procedure that is relevant to the present work. The spectra are computed in a two step process starting with a standard self-consistent ground state calculation followed by an excited state calculation where one electron is removed from the targeted core orbital of a selected atom and is placed in the bottom of the conduction band. The supercell model used in this work is sufficiently large to avoid the core-hole-core-hole interactions between the adjacent cells. Self consistent iterations account for the excited-electron core-hole interaction. Then, dipole transitions that explicitly include the momentum matrix elements are computed according to Fermi's Golden rule between the targeted core orbital from the ground state calculation and the conduction band from the excited state calculation.

In the present work, the HB criterion is based on bond order (BO) calculations using the Mulliken scheme<sup>27</sup> where BOs are computed according to:

$$\rho_{\alpha\beta} = \sum_{n,occ} \sum_{i,j} c_{i\alpha}^{*n} c_{j\beta}^n S_{i\alpha,j\beta} . \quad (1)$$

In eq.(1)  $S$  is the overlap matrix between atoms  $\alpha$  and  $\beta$  with orbitals labeled as  $i$  and  $j$ . The  $C$  values are the eigenvector coefficients of the  $n^{th}$  occupied state. A BO value characterizes the overall bond strength between two atoms and is far more accurate and concise than the purely geometric criteria because it is derived from the quantum mechanical wave function. A minimal basis set (H ( $1s$ ) and O ( $1s$ ,  $2s$ ,  $2p$ )) is used in the BO calculations because the Mulliken scheme is more effective when the basis is more localized.

### III. ELECTRONIC STRUCTURE AND H-BONDING PROPERTIES

The calculated DOS and PDOS plots are displayed in Fig. 4. The model has a HOMO-LUMO gap of about 4.51 eV which is slightly lower than the values obtained by other DFT calculations using LDA and GGA.<sup>28</sup> The element resolved PDOS shows the strongly covalent nature of the bonding between O and H in the H<sub>2</sub>O molecule. It is characterized by a sharp peak at -1.15 eV from the O lone pair and two other peaks at -6.64 eV and -18.68 eV. These valence electronic structures are in good agreement with both the experimental photoelectron spectroscopy (PES) studies<sup>29,30</sup> and the theoretical DFT work by Brancato *et al.*<sup>10</sup>

In a water model, HBs (represented as O...H) are much weaker than the O-H covalent bonds yet they are sufficiently strong to dictate the intermolecular interaction. There have been several criteria proposed for defining an HB. The effective pair potential scheme uses the local minimum in the potential curve as the upper limit of H-bonding energy.<sup>31</sup> The HBs can also be defined by a geometric cutoff using different sets of atomic configuration parameters.<sup>2, 32</sup> The near-neighbor hydrogen and oxygen (NNHO) criterion can be considered as an upgrade of the geometric cutoffs because it is less dependent on rigid arbitrary atomic distances.<sup>33</sup> Finally, the quantum mechanical bond order (BO) values can reflect the stability differences between different kinds of bonds and therefore can help to distinguish HBs.<sup>34</sup>

Fig. 5 displays our results on the BO distribution of (O, H) pairs with  $R_{OH} < 3.5\text{\AA}$ . The distribution range can be divided into three regions. Region I is extremely narrow with many very small BO values, the atoms in this region are considered to be non-bonded. In region III, the distribution has a narrow peak centered at 0.27 originating from covalent O-H bonds within the H<sub>2</sub>O molecules. The HB distribution is in region II. It is well separated from the covalent bonding above and it shows a clear minimum at 0.015 (marked with an arrow) separating it from region I. According to this distribution, the HBs are the O...H pairs with BO values in the range of 0.015 to 0.100 centered approximately at 0.05. The lower end of the distribution constitutes the weak HBs and the high end of the distribution represents the stronger HBs. We have further checked the intermolecular O-H distances of atoms associated with BO values that are less than 0.015, and found that all of them are larger than the well accepted HB separation of 1.98Å in liquid water. In region II, only three HBs have O-H separations that are slightly longer than

1.98Å. This is because the BO value does not simply scale with the distance of separation but is also affected by the bond angle and presence of other nearby atoms.

Fig. 6 illustrates the HBs between a H<sub>2</sub>O molecule and its two nearest neighbor molecules, (H<sub>2</sub>O)' and (H<sub>2</sub>O)". A water molecule (H<sub>2</sub>O) can play two roles in hydrogen bonding, the donor D (with reference to (H<sub>2</sub>O)') and the acceptor A (with reference to (H<sub>2</sub>O)"), depending on which atom is involved in the H bonding. According to our calculated BO values for all the atoms in the model, the 340 water molecules can be divided into four groups with 2, 3, 4, and 5 HBs in which both the donors and acceptors are counted. The group with 4 HBs (2 donors and 2 acceptors or 2D2A) is the fully-bonded group which accounts for 85% of all the HBs. The four HBs in these molecules all tend to have similar strength. Other groups with 2 (1D1A and 2D0A, 3.2%) or 3 (2D1A and 2A1D, 10.3%) HBs have a much smaller presence and are usually identified as broken-bonded. The smallest group (1.5%) with 5 HBs (2D3A) is called the over-bonded group, and it has relatively weak HBs. The average HB number per molecule is 3.85 and this appears to support the tetrahedral HB network model in bulk water. The distributions of the groups with 2, 3, and 5 HBs are shown in Fig.7. For the 2 HB group, the centroid is near the middle with a BO value close to 0.05. For the 3 HB group it shifts to the left indicating a weaker average HB strength for that group. For the 5 HB group, they also tend to be at the region of much smaller BO values. We have compared these electronic structure results with other snapshot configurations obtained from different steps along the equilibrium trajectory of the *ab initio* MD simulation and found that all of them have similar percentages for the four groups. This finding is in contrast with another proposed network model consisting of filamentous H<sub>2</sub>O chains that are formed by H<sub>2</sub>O molecules with two strong HBs each. The chains are said to interact with a surrounding disordered cluster network through weak hydrogen bonding.<sup>2</sup>

In order to have a better understanding of the relationship between hydrogen bonds and the intermolecular configurations and also to compare with other HB criteria, we plotted the intermolecular parameters  $r_{OO'}$  and  $\alpha$  (defined in Fig. 6) of each HB in Fig. 8.. Wernet *et al.*<sup>2</sup> suggested a geometrical cutoff of  $r_{OO'} = -0.00044 \alpha^2 + 3.3 \text{ \AA}$  (curve (i) in Fig.8) to show which parametric combinations permit hydrogen bonding. The discrete data from our model stay well under this curve with the majority in the range of  $r_{OO'} = 2.6\text{-}2.8 \text{ \AA}$  and  $\alpha = 1^\circ\text{-}15^\circ$ . This indicates that the parabolic curve from Ref. 2 is not stringent enough in describing the condition of HB formation. It is highly unlikely for HBs to form with  $r_{OO'}$  larger than 3.1 Å and  $\alpha$  greater than 28°. The scattered plot in Fig. 8 also shows that the most dense population of HB distribution is around  $r_{OO'} = 2.7 \text{ \AA}$  and  $\alpha = 8^\circ$  and that there is no explicit relation between the number of HBs for a molecule and its  $r_{OO'}$  or  $\alpha$ . From the discussion above, we can see that BO criterion is a simple and accurate way to define the presence of HBs.

We have also attempted to identify statistical correlations between the number of HBs for a molecule with the intramolecular parameters  $r_{OH}$  and  $\theta$  ( $r_{OH} = (r_{OH1} + r_{OH2})/2$ ;  $\theta = \angle HOH$  from Fig. 6). In Fig. 9, each data point represents the parameters for one water molecule and they are plotted in accordance with the four groups categorized above. The average  $r_{OH}$  of the broken-bonded HBs (groups i, ii) are mainly distributed in the range of shorter BLs while the full- and over-bonded ones (groups iii, iv) occupy the longer range region. This is reasonable since the molecules with shorter  $r_{OH}$  tend to be more charge localized. It is also clear that the fully-bonded molecules have a wider distribution in  $\theta$  covering both the larger and the smaller ends.

## IV. SPECTROSCOPIC PROPERTIES

We have calculated the O-K edges for *all* 340 oxygen atoms in this large model using the supercell-OLCAO method.<sup>26, 35</sup> The data provides us with a sufficiently large sample of the XANES spectra to investigate meaningful correlation of spectral features with the HB structure of a model closely related to bulk water. Fig. 10(a) shows the experimental X-ray Raman scattering (XRS)<sup>2</sup> and X-ray absorption spectra (XAS)<sup>36</sup> together with our calculated O-K edge averaged over all single spectra. The calculated total spectrum is shifted by 5.99 eV to the left to align with the main peak in the experimental curves. Clearly, our total spectrum shows a pre-edge peak at  $\sim 535$  eV, a shoulder-like structure near 537 eV, a main peak at 538 eV, and a post-edge broad peak between 540 and 541 eV. These features are in very good agreement with experimentally measured spectra.<sup>2</sup> The presence and reproduction of the shoulder-like structure at 537 eV is important and this feature has been routinely neglected by others in discussing their research results.

For better interpretation, the 340 O-K edge spectra are divided into four groups according to the HB numbers and they are shown in Fig. 10(b). It can be seen that the pre-peak originates predominately from the group with 2 HBs with no contribution from the over-bonded group with 5 HBs. This observation is consistent with other findings on the relation between the pre-peak intensity and broken HBs.<sup>37</sup> On the other hand, the post-edge region is more affected by the fully-bonded molecules. Fig. 10(a) also shows that the ratio between the pre-peak and main peak is larger for the experimental curve than for the calculated one. This could be attributed to several factors. First, because of the periodic boundary conditions, the model in this work represents the bulk water with no surface dangling bonds. Therefore it is reasonable to have a smaller portion of broken-bonded water molecules and a higher number of HBs per molecule. Second, the theoretical curve is the superposition of many individual curves with different edge onsets which tends to smooth out the sharp features. This is illustrated in Fig. 11 where we display the 11 O-K edge spectra for the group with 2 HBs, or 3.2% of the total 340 spectra. As can be seen, all have a strong pre-peak but they have different edge onsets and when added together the resultant is a less prominent pre-peak. The difference in their edge onsets is related to their different local geometries in addition to their HB features. Because the position of the edge onset is determined from the difference in total energy of the ground state and the excited state, it is conceivable that a more accurate determination of those energies would slightly reduce the variation and then increase the strength of the pre-peak in the total spectrum. In Fig.12 we randomly selected O-K spectra (molecule number: 39, 328, 201, 255) from each of the groups among the 340 spectra calculated. Generally, as the HB numbers increase the observed trend is that the pre-edge peak height decreases and the post-edge height increases.

## V. CONCLUSIONS

Based on our detailed *ab initio* calculation of a model to mimic bulk water and the use of quantitative bond order values to define HBs, we show that tetrahedrally coordinated water molecules dominate with an average of 3.85 HBs per water molecule. The distances ( $r_{OO'}$ ) and angles ( $\angle O'OH$ ) that characterize the HBs are narrowly confined in the range of 2.6-2.8Å and  $1^\circ$ - $15^\circ$  respectively. Large scale non-*ab initio* calculations could be guided by this more stringent



criterion when interpreting their results. The calculated O-K edge XANES spectra correctly reproduce the peak features observed in the experiments and the decomposition of the spectra according to HB numbers confirms that the pre-peak is caused by H<sub>2</sub>O molecules with fewer than four HBs while the main- and post-peak structures are determined by the local geometry of the individual molecules and their surroundings. This work clearly demonstrates that the *ab initio* BO criterion used to define weak hydrogen bonding is accurate and efficient, and can be applied to complex liquids, cement hydrates, bio-molecular systems, etc. Further, the accurate calculation of many XANES spectra, which are very sensitive to the variations of local atomic environment, can be used to elucidate subtle points of the structural properties of complex materials.

#### ACKNOWLEDGEMENTS

This work is supported by the U.S. Department of Energy under the Grant No DE-FG02-84DR45170. This research used the resources of NERSC supported by the Office of Science of DOE under the contract No DE-AC03-76SF00098.

## References

1. G. A. Lyakhov and D. M. Mazo, *Europhys. Lett.* 57, 396 (2002).
2. P. Wernet, et al., *Science* 304, 995 (2004).
3. A. K. Soper, *J. Phys.: Condens. Mat.* 17, S3273 (2005).
4. M. Leetmaa, K. T. Wikfeldt, M. P. Ljungberg, M. Odellius, J. Swenson, A. Nilsson, and L. G. M. Pettersson, *J. Chem. Phys.* 129, 084502 (2008).
5. M. Odellius, M. Cavalleri, A. Nilsson, and L. G. M. Pettersson, *Phys. Rev. B* 73, 024205 (2006).
6. J. D. Smith, C. D. Cappa, K. R. Wilson, B. M. Messer, R. C. Cohen, and R. J. Saykally, *Science* 306, 851 (2004).
7. T. Tokushima, Y. Harada, O. Takahashi, Y. Senba, H. Ohashi, L. G. M. Pettersson, A. Nilsson, and S. Shin, *Chem. Phys. Lett.* 460, 387 (2008).
8. A. K. Soper, *Chem. Phys.* 258, 121 (2000).
9. P. T. Kiss and A. Baranyai, *J. Chem. Phys.* 131, 204310 (2009).
10. G. Brancato, N. Rega, and V. Barone, *Phys. Rev. Lett.* 100, 107401 (2008).
11. J. M. Sorenson, G. Hura, R. M. Glaeser, and T. Head-Gordon, *J. Chem. Phys.* 113, 9149 (2000).
12. S. Yoo, X. C. Zeng, and S. S. Xantheas, *J. Chem. Phys.* 130, 221102 (2009).
13. L. Martínez, R. Andrade, E. G. Birgin, and J. M. Martínez, *J. Comput. Chem.* 30, 2157 (2009).
14. J. M. Soler, E. Artacho, J. D. Gale, A. J. García, J. Junquera, P. Ordejón, and D. Sánchez-Portal, *J. Phys.: Condens. Mat.* 14, 2745 (2002).
15. G. Kresse and J. Hafner, *Phys. Rev. B* 47, 558 (1993).
16. J. P. Perdew, K. Burke, and M. Ernzerhof, *Phys. Rev. Lett.* 77, 3865 (1996).
17. A. K. Soper and C. J. Benmore, *Phys. Rev. Lett.* 101, 065502 (2008).
18. E. Schwegler, G. Galli, and F. Gygi, *Phys. Rev. Lett.* 84, 2429 (2000).
19. W. Y. Ching, *J. Am. Ceram. Soc.* 73, 3135 (1990).
20. T. Mizoguchi, A. Seko, M. Yoshiya, H. Yoshida, T. Yoshida, W. Y. Ching, and I. Tanaka, *Phys. Rev. B* 76, 195125 (2007).
21. P. Rulis, H. Yao, L. Ouyang, and W. Y. Ching, *Phys. Rev. B* 76, 245410 (2007).
22. T. Mizoguchi, T. Sasaki, S. Tanaka, K. Matsunaga, T. Yamamoto, M. Kohyama, and Y. Ikuhara, *Phys. Rev. B* 74, 235408 (2006).
23. P. Rulis, W. Y. Ching, and M. Kohyama, *Acta Mater.* 52, 3009 (2004).
24. K. Tatsumi, T. Mizoguchi, S. Yoshioka, T. Yamamoto, T. Suga, T. Sekine, and I. Tanaka, *Phys. Rev. B* 71, 033202 (2005).
25. T. Mizoguchi, J. P. Buban, K. Matsunaga, T. Yamamoto, and Y. Ikuhara, *Ultramicroscopy* 106, 92 (2006).
26. W. Y. Ching and P. Rulis, *J. Phys.: Condens. Mat.*, 104202 (2009).
27. R. S. Mulliken, *J. Chem. Phys.* 23, 1833 (1955).
28. V. Garbuio, M. Cascella, L. Reining, R. D. Sole, and O. Pulci, *Phys. Rev. Lett.* 97, 137402 (2006).
29. A. Nilsson, H. Ogasawara, M. Cavalleri, D. Nordlund, M. Nyberg, P. Wernet, and L. G. M. Pettersson, *J. Chem. Phys.* 122, 154505 (2005).
30. D. Nordlund, M. Odellius, H. Bluhm, H. Ogasawara, L. G. M. Pettersson, and A. Nilsson, *Chem. Phys. Lett.* 460, 86 (2008).

31. A. Rahman and F. H. Stillinger, *J. Am. Chem. Soc.* 95, 7943 (1973).
32. R. Kumar, J. R. Schmidt, and J. L. Skinner, *J. Chem. Phys.* 126, 204107 (2007).
33. A. D. Hammerich and V. Buch, *J. Chem. Phys.* 128, 111101 (2008).
34. M. V. Fernández-Serra and E. Artacho, *Phys. Rev. Lett.* 96, 016404 (2006).
35. S.-D. Mo and W. Y. Ching, *Phys. Rev. B* 62, 7901 (2000).
36. S. Myneni, Y. Luo, L. Å. Näslund, M. Cavalleri, and L. Ojamäe, *J. Phys.: Condens. Mat.* 14, L213 (2002).
37. D. Nordlund, H. Ogasawara, K. J. Andersson, M. Tatarkhanov, M. Salmerón, L. G. M. Pettersson, and A. Nilsson, *Phys. Rev. B* 80, 233404 (2009).

## Figure Captions

Fig. 1. The periodic water model with 340 H<sub>2</sub>O molecules.

Fig. 2. (a) Covalent bond length  $r_{OH}$  and (b) bond angle  $\theta$  ( $\angle HOH$ ) distributions.

Fig. 3. Radial pair distribution functions for the water model (red): (a) O-H; (b) H-H; and (c) O-O. The experimental data (cyan) is from Ref. 8.

Fig. 4. (Color on line) Calculated DOS (black solid) and PDOS (blue dash dot: O; red dash: H) in water.

Fig. 5. Distribution of all O and H bonds in the water model: Region I: non-bonded; Region II: H bonded; Region III: covalently bonded.

Fig. 6. Schematic illustration of donor and acceptor H bonds between three water molecules H<sub>2</sub>O, H'<sub>2</sub>O', and H''<sub>2</sub>O''.

Fig. 7. (Color on line) Distribution of the H bonds for the 3 groups which do not have 4 HBs: 2 HB group (blue); 3 HB group (pink) and 5 HB group (yellow). The group with 4 HB dominates (85%) and is similar to the distribution in region II in Fig. 5.

Fig. 8. Scatter plot of  $r_{OO'}$  vs  $\alpha$  ( $\angle O'OH$ ) for all hydrogen bonded OH pairs in the model. The solid line is the curve defining HBs from Ref. 2. Different symbols represent the data from the four different groups with 2, 3, 4, and 5 HBs.

Fig. 9. Scatter plot of the average  $r_{OH}$  vs  $\theta$  within the H<sub>2</sub>O molecule for all 340 H<sub>2</sub>O molecules in the model. Different symbols represent the data from the four different groups with 2, 3, 4, and 5 HBs.

Fig. 10. (a) O-K edge XANES spectra: (i) experimental XRS data for water at 25°C from ref. 2.; (ii) Experimental XAS data for water at ambient conditions from ref. 33; (iii) Averaged spectra over 340 molecules from present calculation. The vertical dotted lines indicate the locations of spectra features. (b) Calculated total spectra for the four categorized groups with 2, 3, 4, and 5 HBs.

Fig. 11. All 11 individual calculated O-K edge spectra in the 2HB coordinated group.

Fig. 12. A typical representative spectrum from each group with 2-5HB (molecule ID#s 39, 328, 201, 255).

Fig. 1

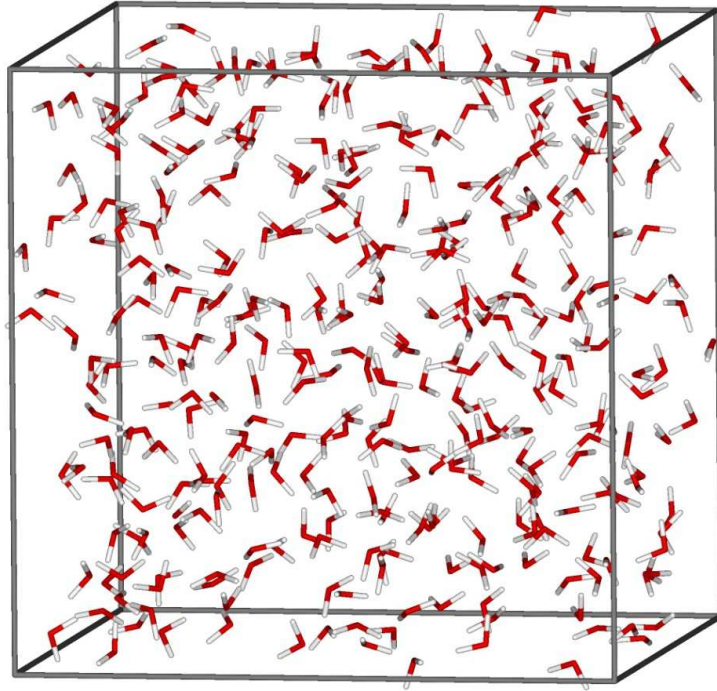


Fig. 2

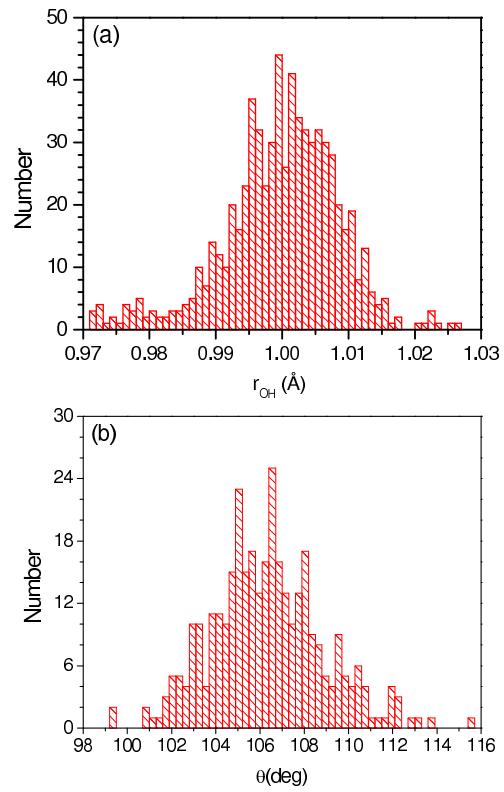


Fig. 3

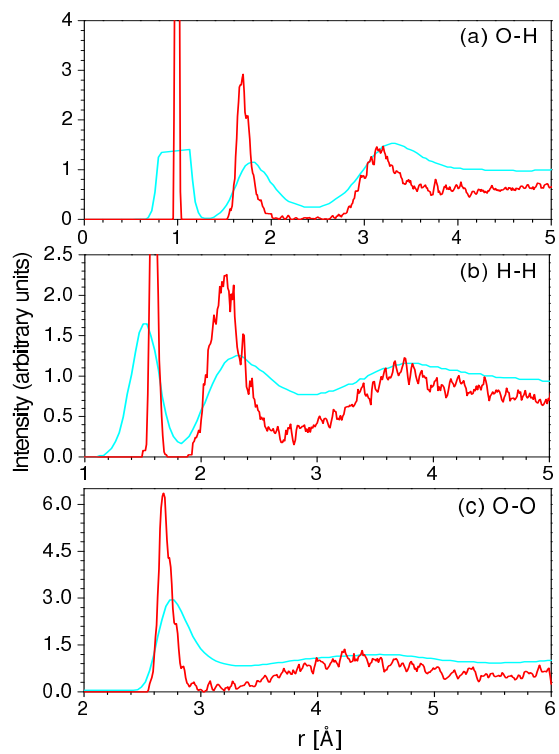


Fig. 4

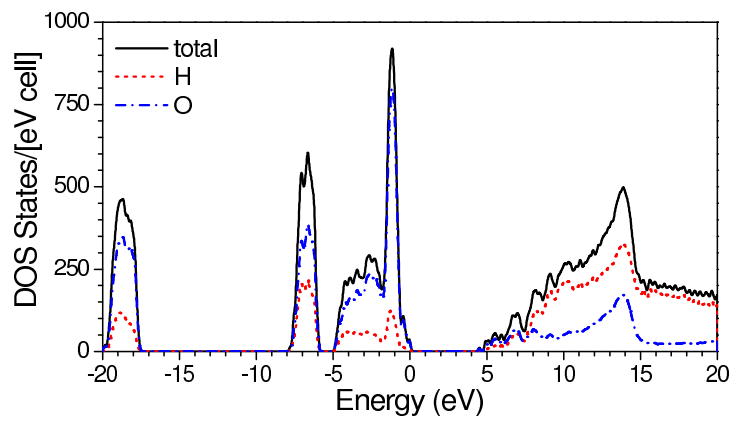




Fig. 5

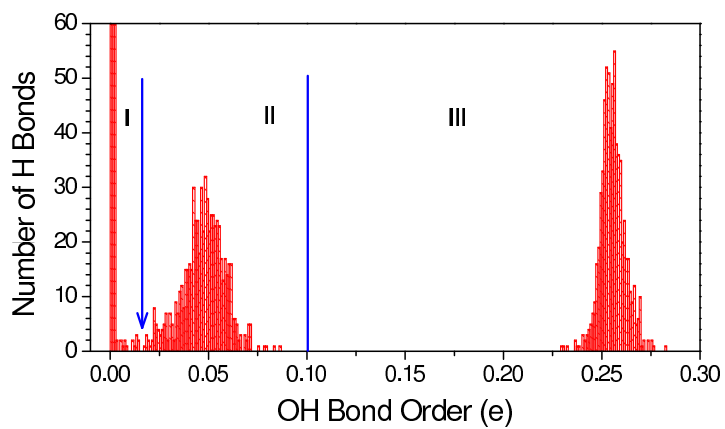


Fig. 6

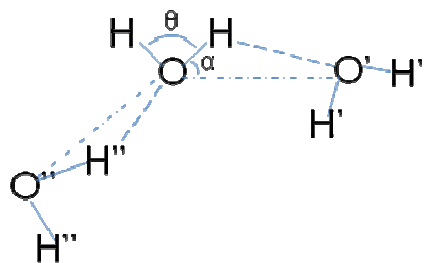


Fig. 7

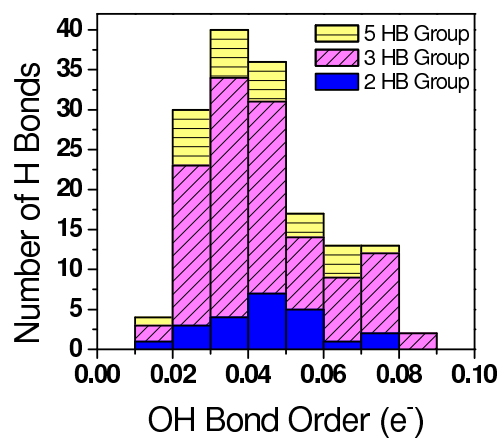


Fig. 8

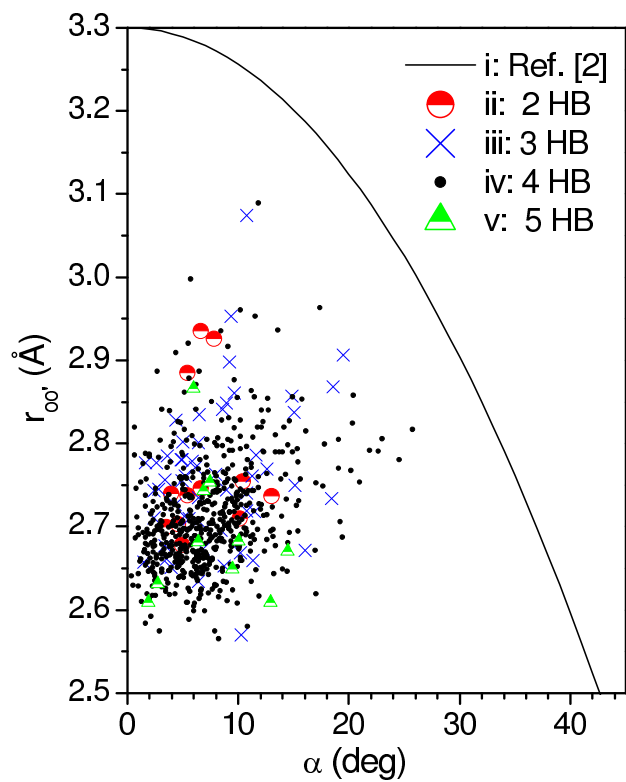


Fig. 9

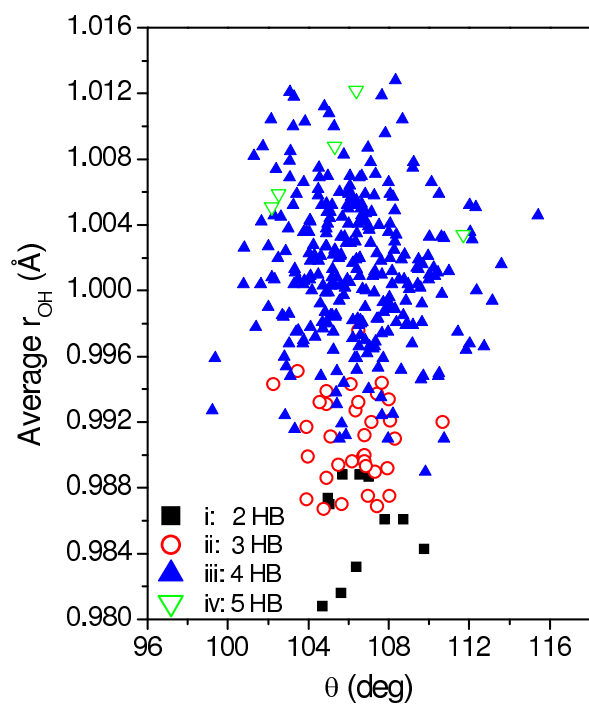


Fig. 10

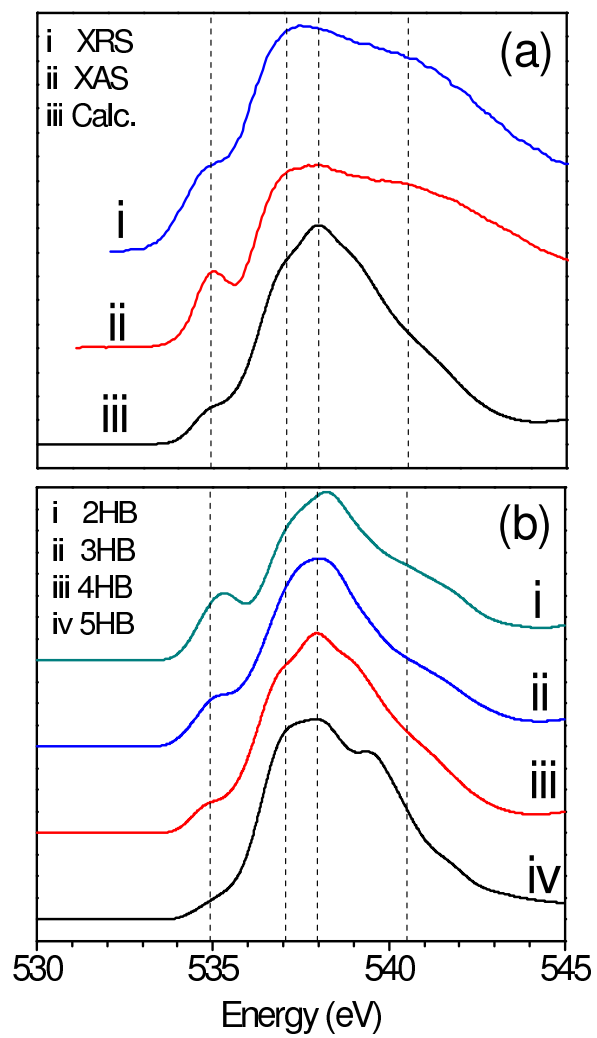


Fig. 11

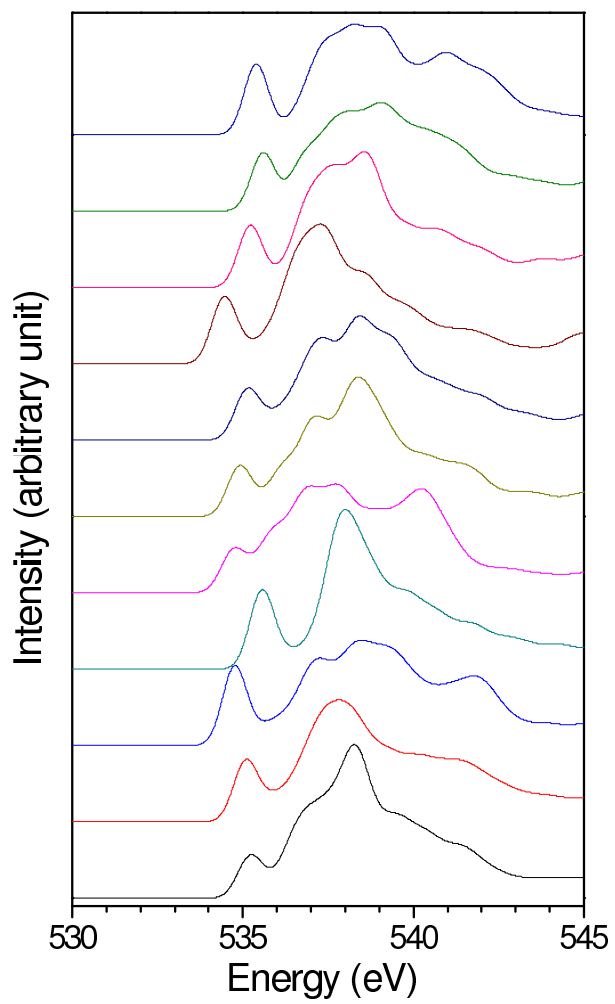


Fig. 12

